



Published in final edited form as:

Biomaterials. 2007 April ; 28(12): 2097–2108.

Enhanced Neurite Growth from Mammalian Neurons in Three-Dimensional Salmon Fibrin Gels

Yo-Ei Ju¹, Paul A. Janmey^{1,2}, Margaret McCormick², Evelyn S. Sawyer³, and Lisa A. Flanagan^{1,4,*}

¹ Division of Experimental Medicine, Brigham and Women's Hospital, Harvard Medical School, Boston, MA 02115

² Department of Physiology and Institute for Medicine and Engineering, University of Pennsylvania, Philadelphia, PA 19104

³ Sea Run Holdings, Inc., 76 Pine St., Freeport, ME 04032

⁴ Department of Pathology, School of Medicine, University of California at Irvine, Irvine, CA 92697

Abstract

Three-dimensional fibrin matrices have been used as cellular substrates *in vitro* and as bridging materials for central nervous system repair. Cells can be embedded within fibrin gels since the polymerization process is non-toxic, making fibrin an attractive scaffold for transplanted cells. Most studies have utilized fibrin prepared from human or bovine blood proteins. However, fish fibrin may be well suited for neuronal growth since fish undergo remarkable central nervous system regeneration and molecules implicated in this process are present in fibrin. We assessed the growth of mammalian central nervous system neurons in bovine, human, and salmon fibrin and found that salmon fibrin gels encouraged the greatest degree of neurite (dendrite and axon) growth and were the most resistant to degradation by cellular proteases. The neurite growth-promoting effect was not due to the thrombin used to polymerize the gels or to any copurifying plasminogen. Co-purified fibronectin partially accounted for the effect on neurites, and blockade of fibrinogen/fibrin-binding integrins markedly decreased neurite growth. Anion exchange chromatography revealed different elution profiles for salmon and mammalian fibrinogens. These data demonstrate that salmon fibrin encourages the growth of neurites from mammalian neurons and suggest that salmon fibrin may be a beneficial scaffold for neuronal regrowth after CNS injury.

1. Introduction

Three-dimensional matrices provide a physiological, deformable substrate for cell growth. Studies dating back to the 1970's demonstrate that the morphology and behavior of cells cultured on or in deformable substrates more closely mimic those of cells *in vivo* [1-3]. In addition to providing a more physiological condition for growth, three-dimensional matrices can also be used to bridge sites of injury. In these cases, the matrix material can serve as a scaffold for cells, which are either transplanted with the matrix or ingrowing from the damaged tissue, and as a source of exogenous growth factors or extracellular matrix molecules.

*Address correspondence to: Lisa A. Flanagan, Ph.D., Department of Pathology, School of Medicine, University of California at Irvine, D440 Medical Sciences I, Irvine, CA 92697-4800, Tel: (949) 824-5786, Fax: (949) 824-2160, Email: lflanaga@uci.edu

Publisher's Disclaimer: This is a PDF file of an unedited manuscript that has been accepted for publication. As a service to our customers we are providing this early version of the manuscript. The manuscript will undergo copyediting, typesetting, and review of the resulting proof before it is published in its final citable form. Please note that during the production process errors may be discovered which could affect the content, and all legal disclaimers that apply to the journal pertain.

Trauma to the mammalian central nervous system can result in gaping lesions that may benefit from a bridging three-dimensional matrix [4,5]. For example, injury to the human spinal cord results in a cystic cavity and a glial (astrocyte) scar that prevent regrowth of neuronal axons, thereby prohibiting recovery from the motor and sensory deficits associated with the injury. Ideally, a bridging material would stimulate axonal extension across the cavity, while limiting the processes that lead to astrocyte proliferation. Polymerization *in situ* would also be advantageous so that cells can be embedded in the matrix and the matrix surface can be tightly apposed to the surrounding tissue. In addition, the material should be biodegradable and should match the compliance (stiffness) of the host tissue. For example, fairly compliant (easily deformable but not fluid) matrices encourage the greatest rate of neurite extension and branch formation from neurons [6,7]. Compliant matrices also discourage astrocyte growth and should reduce glial scar formation *in vivo* [8,9]. Additionally, the ability to incorporate growth factors and extracellular matrix molecules into the matrix would offer the opportunity to optimize the biochemical, as well as the physical, milieu.

Fibrin is a physiologic, three-dimensional matrix that fulfills these criteria. Fibrin formation is non-toxic and occurs during the coagulation cascade when fibrinogen (FBG) is cleaved by thrombin to form fibrin monomers, which then spontaneously polymerize to form a three-dimensional matrix (for a recent review see [10]). Factor XIII, when activated to the transglutaminase Factor XIIIa, covalently cross-links fibrin monomers to form a durable matrix that can be degraded by specific molecules, most notably plasmin. The compliance and polymerization rate of fibrin can be tightly controlled by varying the concentration of FBG and thrombin, respectively. Recent studies show that lower concentrations of FBG can be used to form fibrin with compliance similar to those of matrices that encourage neurite extension and branching [6-8]. Exogenous ligands beneficial for repair, such as growth factors and extracellular matrix molecules, can be covalently crosslinked to fibrin by Factor XIIIa [11].

Fibrin has been successfully utilized in repair strategies for a variety of *in vivo* neuronal injury models. Fibrin has been used as a glue to attach other grafting materials (e.g. [12]), as a matrix to provide delivery of neurotrophic factors [13,14], and as a scaffold for transplanted cells or to fill implanted guidance channels [15-17]. In each of these cases, fibrin was prepared from FBG and thrombin isolated from bovine or human sources. However, mammalian fibrin gels degrade rapidly [5,18,19] and may be contaminated with blood-borne pathogens such as HIV, hepatitis C, and prion proteins. The limitations of mammalian fibrin have led to the preparation of fibrins from other species as cellular substrates. A recent study tested fibrin prepared from salmon proteins and found that endothelial cell capillary tube sprout formation was greater in salmon fibrin than human fibrin [19]. Although salmon and human fibrin function similarly [20], there may be subtle differences in the salmon and human proteins that make up fibrin. For example, the pattern of FBG subunits resolved by SDS-PAGE is different for salmon and human FBG and the polymerization of salmon fibrin is less affected by high pH and salt than human fibrin [20]. The fish central nervous system has a remarkable capacity for repair (e.g. [21]), and regeneration is associated with upregulation of the fibrin-associated molecule Factor XIIIa [22,23]. Salmon fibrin may also be safer for transplants since known salmon viruses are not transmissible to mammals [24]; in part because fish are coldwater animals and most viruses that infect them are typically inactivated at human body temperature.

The potential benefits of salmon fibrin led us to test its utility as a three-dimensional substrate for central nervous system (CNS) neurons. We compared the growth of several types of primary neurons (mouse spinal cord, mouse cortical, and rat cortical) in three-dimensional bovine, human, and salmon fibrin. As a control, we also cultured neurons in Matrigel, a commonly used three-dimensional matrix enriched in laminin and collagen. Our data show that salmon fibrin encourages greater neurite extension than mammalian fibrin and that salmon fibronectin and FBG/fibrin are involved in this effect.

2. Materials and Methods

2.1 Protein preparation

Salmon (*Salmo salar*) thrombin was prepared as previously described [25]. Salmon fibrinogen (FBG) was prepared using the ammonium sulfate purification method previously described [20]. Fibronectin and plasminogen were removed from FBG by gelatin and L-lysine chromatography [26,27]. The final concentration of FBG in all preparations was determined by optical density using an extinction coefficient of $e(1\%, 280\text{ nm}) = 16.4$ or by Bradford assay. FBG preparations were assayed for endotoxin levels by LAL assay, and only preparations with levels below 0.5 EU/ml were used for cell culture. Purified salmon FBG and thrombin preparations were lyophilized and stored at -80°C . Bovine and human FBG and thrombin were obtained as lyophilized proteins from Calbiochem or Sigma and had endotoxin levels less than 0.5 EU/ml.

Lyophilized FBG (salmon, bovine, or human) was rehydrated to generate a 50 mg/ml FBG solution (after rehydration, the buffer for bovine and human FBG was 20 mM citrate-HCl, pH 7.4 and for salmon FBG was 50 mM Tris, 150 mM NaCl, pH 7.4). Salmon FBG was kept at room temperature (with gentle mixing) during rehydration, while both mammalian FBG solutions required heating at 37°C to completely dissolve. After rehydration, FBG solutions were filter sterilized (0.2 μm). Protein determinations of sterilized FBG solutions showed that very little protein was lost on the filters, even when solutions had clogged the filters. In some cases, rehydration of FBG to a concentration of 50 mg/ml approximately doubled the salt concentration of the solution. However, control experiments showed that the increase in salt concentration had no effect on gel polymerization, cell growth, or gel degradation. Lyophilized thrombins were rehydrated to a final concentration of 100 U/ml in PBS and were filter sterilized. Aliquots of sterile proteins were stored at -80°C . Immediately prior to use, aliquots were thawed on ice (salmon FBG and thrombins from all species) or at 37°C (bovine and human FBG). The plasmin inhibitor, ϵ -amino-n-caproic acid (ϵ -ACA, 2.5 M in PBS, filter sterilized) was added to bovine and human FBG at a final concentration of 50 mM. Matrigel (BD Biosciences) was thawed on ice to prevent premature polymerization.

2.2 Neuron culture

Primary spinal cord and cortical mouse neurons were obtained from E13.5 embryos (C57Bl6) and cultured in Mouse Neuron Medium as previously described [7]. Rat (Sprague-Dawley) cortical neurons were isolated from E18 cortices obtained from Brain Bits, LLC and cultured using manufacturer's protocols in Rat Neuron Medium (Neurobasal with B27 supplement, 0.5 mM glutamine, 25 μM glutamate; all components from Gibco/Invitrogen)[28].

Neurons were embedded in salmon, bovine, and human fibrin gels using the following procedure. FBG (final concentration 3 mg/ml) and cells (final concentration 50,000-300,000 cells/100 μl) were diluted in Mouse Neuron Medium. Thrombin was added to a final concentration of 1.5 U/ml to stimulate polymerization. In some cases the FBG concentration was 2.5 mg/ml or the thrombin concentration was 2.0 U/ml with similar results. After gentle mixing, 100 μl of gel solution with cells was rapidly transferred to a poly-D-lysine (0.52 $\mu\text{g}/\text{cm}^2$ for 5 minutes then rinsed with water) coated coverslip or one well of a 4-well chamber slide (Nunc) and polymerized at room temperature for ~ 20 minutes. Comparisons of gel formation in different cell culture media showed that polymerization was more efficient in media containing ~ 1.8 mM calcium (such as EMEM and DMEM) than in those with ~ 1.0 mM calcium (such as DMEM/F12). Neurons were embedded in Matrigel using the same procedures as for fibrin gels except that neurons were mixed with ice-cold, undiluted Matrigel and polymerization was stimulated by allowing the solution to warm to room temperature. After polymerization, all gels were covered with neuronal culture medium (Mouse Neuron

Medium for mouse spinal cord and cortical neurons and Rat Neuron Medium for rat cortical neurons) and kept in a humidified 37°C, 5% CO₂ incubator. For some experiments echistatin (2 µM final concentration, Sigma) was added with the culture medium after gel polymerization. For control cultures, neurons were plated directly on glass coverslips treated with laminin (coverslips pretreated for 5 minutes with poly-D-lysine then incubated with laminin (BD Biosciences), 20 µg/ml (5 µg/cm²) in EMEM, overnight in a 37°C, 5% CO₂ humidified incubator). Coverslips were rinsed with PBS prior to use. Live cells in the gels were visualized with a Nikon TS100 inverted phase contrast microscope and images captured with a Nikon CoolPix 950 digital camera. Whole gels were visualized with a Nikon SMZ1500 stereo dissecting microscope and images captured with a Spot RT CCD camera and software (Diagnostic Instruments, Sterling Heights, MI).

2.3 Immunostaining and neurite analysis

After 2-7 days in culture, the cells and gels were fixed with paraformaldehyde (4% paraformaldehyde, 5 mM MgCl₂, 10 mM EGTA, 4% sucrose in PBS; the sucrose was omitted for fixation of cells in Matrigel). Immunostaining followed usual protocols [29,30] except that incubation times were increased to allow diffusion through the gels and all incubations were on a rocking platform (blocking step overnight at 4° C, primary antibody overnight at 4° C, secondary antibody for 3 hours at room temperature). Antibodies were as follows: anti-class III beta-tubulin (TuJ1) polyclonal, 1:5000 (Research Diagnostics, Flanders, NJ); anti-NFH (phosphorylated neurofilament H) (SMI31) monoclonal, 1:50 (Sternberger Monoclonals, Lutherville, MD); anti-GFAP (glial fibrillary acidic protein) polyclonal, 1:1000 (Chemicon, Temecula, CA); anti-Map5/Map1b (microtubule associated protein 5)(AA6) monoclonal, 1:200 (Sigma, St. Louis, MO). Secondary antibodies were anti-rabbit or anti-mouse IgG coupled to fluorophores (Jackson ImmunoResearch, PA). Nuclei were stained with Hoechst 33342, 2 µg/ml in PBS (Molecular Probes, Eugene, OR). Immunostained cells in the gels were viewed on a Nikon E600 epifluorescence microscope and images of labeled cells captured with a Spot RT CCD camera and software (Diagnostic Instruments, Sterling Heights, MI). Images were processed and compiled using Adobe Photoshop (Adobe Systems, San Jose, CA) (neurites that extended along the z-axis in the gels were imaged at multiple focal planes and overlapping images reconstructed into flattened montages in Photoshop). Total neurite length per cell was quantified by measuring the length of all neurites and branches for cells with clearly identifiable cell bodies. NIH Image (or ImageJ) was used to make measurements and data were analyzed and graphed with KaleidaGraph (Synergy Software, Reading, PA). Unless otherwise stated, neurite length was measured after 3 days culture in the gels. Quantitative data were obtained from 10 or more neurons per gel and n=3 or more independent experiments. Unpaired Student's t-test was used for statistical analyses.

2.4 Analysis of gel compliance

The compliance of the different gels was determined by measuring the shear storage moduli (G') of gels prepared with the same buffer conditions used for cell culture, but without embedded cells. Measurements were made with a RFS3 fluid rheometer (Rheometrics, Piscataway, NJ) using a maximal strain amplitude of 2% at a frequency of 10 rad/s. Detailed methods are provided elsewhere [8].

2.5 Ion exchange chromatography and SDS-PAGE

DEAE Sephadex A-25 beads (Sigma, St. Louis, MO) were allowed to swell for 48 hours in PBS pH 7.4 at room temperature then loaded into an FPLC HR 10/10 column with an internal diameter of 10 mm and a column length of 100 mm. Human (Calbiochem) and salmon FBG were diluted to 5 mg/ml and dialyzed overnight at 4°C against phosphate-EDTA buffer (50 mM sodium phosphate pH 7.4, 10 mM sodium-EDTA)[31]. The DEAE column was loaded

with 1 ml of either human or salmon FBG with a flow rate of 2 ml/min and collection of 2 ml fractions. The column was washed with phosphate-EDTA buffer and after 20 min, a gradient of 0-0.2 M NaCl was used to elute FBG. Afterwards, the NaCl concentration was increased rapidly to 1.0 M to remove any tightly bound protein. The absorbance of each fraction was measured at 280 nm using an Eppendorf BioPhotometer. Between samples of human and salmon FBG, the column was washed with 2 M NaCl, 0.1 M NaOH and re-equilibrated with phosphate-EDTA buffer. The eluted peak fractions of salmon fibrinogen were separated by SDS-PAGE (10% polyacrylamide gel, 5 μ g total protein per well) and stained with coomassie.

3. Results

Primary neurons isolated from embryonic mice or rats were combined with FBG and thrombin to embed neurons within three-dimensional fibrin gels. We used a concentration of FBG shown to produce fibrin of optimal compliance for neurite growth [6,7,32] but not permissive for astrocyte growth [8]. Control experiments showed that treatment of neurons on coverslips with thrombin at the concentrations used for gel formation was not toxic and did not alter neurite growth. The dimensions of the polymerized fibrin gels were \sim 8 mm diameter, \sim 3 mm height. Neurons cultured in the gels for several days extended neurites until fixation for immunostaining and analysis. Neurites could be tracked across multiple focal planes, confirming that they were growing through the three-dimensional matrix in the Z-axis, rather than along the gel surface or the underlying coverslip (Fig 1A). Immunostaining for GFAP confirmed that although astrocytes were detected in the same cultures grown on glass, they were not present in the fibrin gels, presumably due to the compliance of the fibrin matrix (data not shown, [8]).

Fibrin can be degraded by enzymes secreted from cells and previous studies have shown that human umbilical vein endothelial cells degrade human fibrin more rapidly than salmon fibrin [19]. In order to assess degradation by neuronally secreted proteases [33,34], fibrin gels from the different species were seeded with equal numbers of mouse spinal cord neurons and grown in identical media and culture conditions. Control experiments showed that fibrin gels from the three species did not degrade when incubated with the culture media alone for up to 7 days. When seeded with cells, human fibrin showed signs of degradation after just a few days of culture, and the gels were almost completely digested after approximately one week (Fig 1B). Bovine fibrin was more resistant, with initial degradation occurring after approximately 5-6 days (data not shown). In contrast, salmon fibrin remained intact for up to 2 weeks, the longest time point measured although salmon fibrin can be degraded by mammalian plasmin [35]. Seeding the gels with mouse or rat cortical neurons resulted in similar patterns of degradation (data not shown). Degradation of the mammalian gels could be slowed by the addition of the plasmin inhibitor ϵ -amino-n-caproic acid (ϵ -ACA), although these gels still degraded more rapidly than the salmon gels. For example, while human fibrin with ϵ -ACA was stable at 6 days, degradation was evident after two weeks, a time point at which salmon fibrin with ϵ -ACA was still intact. In order to control for differences in degradation, subsequent experiments assessing neurite growth in all types of fibrin were carried out in the presence of ϵ -ACA and employed short culture times (1-3 days) before degradation of any of the gels.

Neurite growth in fibrin was initially analyzed by culturing primary E13.5 mouse spinal cord neurons in salmon, bovine, or human fibrin followed by immunostaining to visualize neurites. Neurons in salmon fibrin exhibited significantly longer neurites than those in bovine or human fibrin (Fig 2A). After several days in culture, neurons in salmon fibrin had long neurites that appeared to be axons based on length and morphology (e.g. Fig 1A). Immunostaining with antibodies to phosphorylated neurofilament H subunit, which stains axons but not dendrites, confirmed that these long neurites were axons (Fig 2A).

In order to determine whether the effect on neurite growth was neuronal cell-type specific, we isolated neurons from E18 rat cortex and E13.5 mouse cortex and seeded them into the three types of fibrin. The results were similar to those obtained with mouse spinal cord neurons; cortical neurons from rat (Fig 2B) and mouse extended longer neurites in salmon fibrin than in mammalian fibrin. To quantify neurite growth, we imaged neurites across focal planes, flattened the images into montages, and measured the length of all the cell's neurites to determine total neurite length per cell. All three types of neurons had greater neurite growth in salmon fibrin than in mammalian fibrin (Fig 2C). We also compared fibrin to Matrigel, a secreted extracellular matrix made up of collagen, laminin, and a variety of other components that is often used as a three-dimensional matrix. Neurite growth in Matrigel was similar to that in mammalian fibrin gels and less than that in salmon fibrin (Fig 2C).

Previous studies have shown that the compliance of a three-dimensional matrix can influence neurite growth. Therefore, we assessed the compliance of fibrin and Matrigel by measuring the shear modulus of each of the gels with a plate rheometer. Gels were prepared without implanted cells for these experiments in order to compare the scaffolds to each other directly. All the moduli were relatively similar and within the range of compliances found to be optimal for neurons (~40 to 300 Pa; [6-8]), and the minor variance in compliance did not correlate with the amount of neurite growth in the different matrices (Fig 3A). Thus, the differences in neurite growth cannot be attributed to variability in the compliance of fibrin from different species.

The protein components of fibrin include thrombin, FBG, and several proteins that copurify with FBG and might affect neurite growth. In order to determine whether the type of thrombin influenced neurite growth in fibrin, we prepared fibrin gels from salmon FBG and salmon, human, or bovine thrombin. All three types of thrombin efficiently polymerized the salmon FBG, and neurite growth was similar in the gels (Fig 3B top panels, Fig 3C). The complementary experiment, in which mammalian FBGs were polymerized with salmon thrombin, showed that salmon thrombin was able to polymerize both human and bovine FBG. Again, neurite growth in these gels appeared similar regardless of thrombin source (Fig 3B bottom panels, Fig 3C). Therefore, the increased neurite growth seen in salmon fibrin is due to the salmon FBG or copurifying proteins, not salmon thrombin.

Two proteins that often co-purify with FBG and have been shown to influence neurite growth are fibronectin (FN) and plasminogen [36,37]. Salmon FBG was further purified using affinity chromatography to sequentially remove these two proteins, and neurons were embedded in fibrin prepared from the purified FBGs. Removal of FN and plasminogen decreased the neurite growth-promoting activity of salmon FBG, although the neurite length was still greater than that in mammalian fibrin (Fig 4A, B). Removal of FN alone resulted in levels of neurite growth similar to that in fibrin lacking both FN and plasminogen, suggesting that plasminogen does not contribute significantly to neurite growth (Fig 4B). Analysis by neuronal subtype revealed that mouse spinal cord neurons, compared to mouse cortical and rat cortical neurons, were most affected by the removal of FN (Fig 4C).

Factor XIIIa often copurifies with mammalian FBG, and previous studies of salmon FBG purified by ethanol precipitation showed evidence of copurifying Factor XIIIa [20]. However, salmon FBG purified using ammonium sulfate, rather than ethanol, appears to lack Factor XIIIa since there is no evidence for the formation of dimers generated by transglutamination of the FBG gamma chain ([38] and confirmed in this study (data not shown)). The FBG used to prepare salmon fibrin gels in the current study was purified using ammonium sulfate and these gels support robust neurite growth (e.g. Fig 2), suggesting that Factor XIIIa is not likely to be responsible for the enhanced neurite growth in salmon fibrin.

To assess more directly the role of FBG in the neurite growth-promoting effect of salmon fibrin, we disrupted the interaction of cell-surface integrins with FBG/fibrin. We refer here to FBG/fibrin collectively since during polymerization FBG is cleaved to form fibrin monomers that retain integrin binding sites. Integrins physically link cells to the extracellular matrix and stimulate a variety of signalling cascades, including those regulating cell migration and neurite extension [39]. FBG/fibrin-integrin binding was blocked with echistatin, a disintegrin that disrupts RGD-binding integrins and has the greatest affinity for the $\alpha V\beta 3$ integrin that binds FBG/fibrin and the $\alpha 5\beta 1$ FN-binding integrin [40]. Control experiments showed that mouse spinal cord neurons plated on laminin, which binds RGD-independent integrins, had equivalent neurite growth in the presence and absence of echistatin, confirming that echistatin is specific for particular integrins and not toxic to neurons. In contrast, the adhesion of neurons or neural stem cells to FN-coated coverslips was completely inhibited by echistatin, confirming its efficacy ([30] and data not shown). Mouse spinal cord neurons in FN-free salmon fibrin that were treated with echistatin showed significantly decreased neurite growth when compared to controls (Fig 5). Since these gels lacked FN, the inhibition of neurite outgrowth by echistatin points to the involvement of FBG/fibrin- $\alpha V\beta 3$ linkages. Echistatin treatment of neurons in FN-containing salmon fibrin decreased neurite outgrowth to similar levels as those without FN, which is consistent with inhibition of both $\alpha V\beta 3$ (FBG/fibrin-binding) and $\alpha 5\beta 1$ (FN-binding) integrins by echistatin (data not shown). Echistatin also decreased neurite growth in bovine fibrin (Fig 5B).

Fibrin and its function in the coagulation cascade are generally well conserved across species. However, subtle differences in the human and salmon FBG proteins may exist. We compared human and salmon FBG using DEAE ion exchange chromatography, following the methods of Mosher and Blout [31]. As shown previously, human FBG elutes in three distinct peaks (Fig 6A) that do not correspond to the three chains of FBG but instead each contain intact, but heterogeneous, FBG variants with different affinities for the matrix due to minor variations in protein sequence, glycosylation, degradation, and other modifications [31]. Salmon FBG variants eluted similarly (Fig 6A), but the peaks differed in relative magnitude. Most notably, the weakest bound population eluting at lowest ionic strength was greater for human than for salmon FBG. This difference is consistent with significantly lower isoelectric points of some of the salmon FBG chains revealed by 2-D gel electrophoresis [35]. SDS-PAGE analysis confirmed that the peaks of eluted salmon FBG, like those of human FBG, contained intact protein (Fig 6B).

4. Discussion

By comparing neuronal growth in fibrin from different species, we have found that several different types of neurons (mouse cortical, rat cortical and mouse spinal cord) embedded in salmon fibrin extend longer neurites than those in mammalian fibrin or Matrigel and that these neurons degrade mammalian fibrin more rapidly than salmon fibrin. The effects of salmon fibrin on neurite extension are not due to salmon thrombin, plasminogen, or Factor XIIIa. Instead, salmon FN and FBG/fibrin are primarily involved in neurite growth promotion.

Removal of the adhesion molecule FN from salmon fibrin decreases total neurite length per cell by ~35% (Fig 4). Notably, the neurite growth in FN-free salmon fibrin was still significantly greater than that in the mammalian fibrins (as shown in Fig 4, the total neurite length for neurons in FN-free salmon fibrin is ~2-fold greater than that for neurons in bovine or human fibrin). These data suggest that additional components of salmon fibrin are involved in the neurite growth promotion. A role for FBG is suggested by experiments showing that neurite growth in FN-depleted salmon fibrin treated with echistatin (to block FBG/fibrin-integrin binding) was reduced ~54%. Furthermore, echistatin disruption of integrins that bind FN and FBG decreased neurite growth further than depletion of FN alone (Figs 4 and 5; total

neurite length per cell was reduced ~35% with depletion of FN and ~66% with echistatin treatment). These data suggest that salmon FBG/fibrin aids in the promotion of neurites in salmon fibrin. Echistatin treatment does not abolish all neurite growth in fibrin, which attests to the fact that it is not generally toxic to cells and suggests that some neurite growth occurs via charge-charge or other non-RGD dependent interactions between neurons and the matrix. Echistatin treatment does not cause an equal decrease in the neurite growth in salmon and mammalian fibrin; integrin inhibition results in an ~3-fold decrease in total neurite length in salmon fibrin but only an ~2-fold decrease in bovine (Fig 5). Since the gels have the same FBG/fibrin content, this difference suggests that the integrin-FBG/fibrin affinity or the signalling cascades stimulated by integrin binding may be different for salmon and bovine proteins.

RGD sequences in both FN and FBG are involved in their binding to cell surface integrins, and there may be differences in the number or location of these sequences in the salmon proteins. While no sequence data is available for salmon FN or FBG, the genomes of zebrafish (*Danio rerio*) and pufferfish (*Tetraodon nigroviridis*), which are teleost fish like salmon, have been sequenced and may provide clues to the salmon protein structure. FN usually exists as a dimer and, although it is encoded on a single gene in humans, alternative splicing can generate up to 20 different isoforms in humans. FN has a complex array of multiple different integrin interaction sites, some of which differ between zebrafish and mammals [41]. While one FN gene has been identified in mammals and a similar gene described in zebrafish, a recent report details a second FN gene in zebrafish [41]. Due to the high degree of alternative splicing, a detailed analysis of FN transcripts or proteins from fish will be necessary to determine structural variations that may account for species differences in FN function.

FBG is a large, complex glycoprotein made up of pairs of three chains termed A α , B β , and γ . A comparison of the amino acid sequences of fish (zebrafish and pufferfish) and mammalian (human and bovine) FBG shows differences in the location and number of RGD sequences. Both the human and bovine FBG A α chains encode two RGD sequences, whereas the zebrafish FBG A α contains only one of the two and the pufferfish chain lacks both. In contrast, the human and bovine γ chains have no RGD motif, but the zebrafish and pufferfish γ chains each have one. Assuming similar assembly of the mammalian and fish chains to form functional FBG, the human and bovine proteins would have four RGD sequences, all on the A α chains, zebrafish FBG would have four (two on the A α chain and two on the γ chain), and pufferfish FBG would have two on the γ chain. The differences in the location of RGD sequences may affect accessibility for binding to cellular integrins and may be involved in differential integrin activation, which could in turn influence neurite growth. Other minor variations in the sequences of the FBG chains may also modulate the binding of the RGD region to integrins. For example, the affinity of echistatin for the $\alpha 5 \beta 1$ integrin can be selectively altered by changing a single amino acid near the RGD sequence from Met to Leu [40]. The complexity of the FBG molecule has thus far made it difficult to express recombinant FBG, unfortunately precluding studies such as site-directed mutagenesis of RGD motifs.

FBG chains are extensively post-translationally modified, including the addition of carbohydrates that are likely to differ between mammals and fish. Variations in post-translational modifications such as carbohydrates would influence the charge of FBG and may underlie the different interactions of the salmon and human proteins with anion exchange media (Fig 6) and their different isoelectric points revealed by 2D gel electrophoresis [35]. Elements of FBG structure or post-translational modifications may also modify proteolytic sites and influence the degradation rates of human and salmon fibrin (Fig 1). Interestingly, the predicted N-glycosylation sites of the human, bovine, zebrafish, and pufferfish B β and γ chains are remarkably similar. Differences in carbohydrate modification of the mammalian and fish FBGs may not be based on number or location of glycosylation sequences, but rather on the nature

of the modification. For example, both salmon and trout antithrombins have different sialylated oligosaccharides than the human protein [42]. Carbohydrate can also affect FBG solubility [43], which may be related to the fact that salmon FBG goes into solution at room temperature or 4°C while mammalian FBG requires heating to 37°C to dissolve. Further studies will be necessary to clarify what specific elements of the salmon FBG affect neurite growth and matrix degradation by cellular proteases. Additionally, although our data point to the roles of salmon FN and FBG/fibrin in the promotion of neurite growth, we cannot rule out the possible involvement of other, unidentified FBG-associated molecules that also influence neurite growth.

A recent publication has assessed the immunological consequences of implanting salmon fibrin intraperitoneally in mammals [35]. A single administration of salmon fibrin led to the production of only low titers of antibodies to the salmon proteins. Animals exposed to salmon fibrin multiple times produced high concentrations of antibodies against the salmon proteins, but did not form antibodies that cross-reacted with host proteins. Importantly, coagulation times and fibrin clot strength were normal in animals that produced antibodies to the salmon proteins, showing that the host coagulation system was unaffected. These studies are an important step in assessing the utility of salmon fibrin for human tissue engineering.

Conclusion

Fibrin is beneficial in neural repair strategies in part because its polymerization is non-toxic, it forms compliant matrices, and growth factors and adhesion molecules can be incorporated into the matrix. In this study, we found that fibrin from different species are not equivalent, and that salmon fibrin encourages greater neurite growth and is more resistant to proteolysis than mammalian fibrins. The promotion of neurite growth involves the interaction of neurons with the salmon adhesion proteins FN and FBG/fibrin. These data, coupled with recent studies demonstrating low toxicity of salmon fibrin implanted in animals [35], suggest that salmon fibrin may be a particularly useful biomaterial for treatment of central nervous system injuries.

Supplementary Material

Refer to Web version on PubMed Central for supplementary material.

Acknowledgements

The authors would like to thank Xun Cheng, Stephen Huo, and Steve Marchenko for assistance with three-dimensional neurite measurements, Julia Herod for salmon protein purification, and Ed Monuki for critical reading of the manuscript. This work was supported in part by NIH-NINDS SBIR NS48734 and all animal studies in this paper have been approved by the Institutional Animal Care and Use Committee at the University of California, Irvine.

References

1. Bard JB, Hay ED. The behavior of fibroblasts from the developing avian cornea. Morphology and movement in situ and in vitro. *J Cell Biol* 1975;67(2PT1):400–18. [PubMed: 1194354]
2. Discher DE, Janmey P, Wang YL. Tissue cells feel and respond to the stiffness of their substrate. *Science* 2005;310(5751):1139–43. [PubMed: 16293750]
3. Giannone G, Sheetz MP. Substrate rigidity and force define form through tyrosine phosphatase and kinase pathways. *Trends Cell Biol* 2006;16(4):213–23. [PubMed: 16529933]
4. Geller HM, Fawcett JW. Building a bridge: engineering spinal cord repair. *Exp Neurol* 2002;174(2):125–36. [PubMed: 11922655]
5. Novikova LN, Novikov LN, Kellerth JO. Biopolymers and biodegradable smart implants for tissue regeneration after spinal cord injury. *Curr Opin Neurol* 2003;16(6):711–5. [PubMed: 14624081]
6. Balgude AP, Yu X, Szymanski A, Bellamkonda RV. Agarose gel stiffness determines rate of DRG neurite extension in 3D cultures. *Biomaterials* 2001;22(10):1077–84. [PubMed: 11352088]

7. Flanagan LA, Ju YE, Marg B, Osterfield M, Janmey PA. Neurite branching on deformable substrates. *Neuroreport* 2002;13(18):2411–5. [PubMed: 12499839]
8. Georges PC, Miller WJ, Meaney DF, Sawyer ES, Janmey PA. Matrices with compliance comparable to that of brain tissue select neuronal over glial growth in mixed cortical cultures. *Biophys J* 2006;90(8):3012–8. [PubMed: 16461391]
9. Woerly S, Doan VD, Sosa N, de Vellis J, Espinosa-Jeffrey A. Prevention of gliotic scar formation by NeuroGel allows partial endogenous repair of transected cat spinal cord. *J Neurosci Res* 2004;75(2):262–72. [PubMed: 14705147]
10. Mosesson MW. Fibrinogen and fibrin structure and functions. *J Thromb Haemost* 2005;3(8):1894–904. [PubMed: 16102057]
11. Sakiyama SE, Schense JC, Hubbell JA. Incorporation of heparin-binding peptides into fibrin gels enhances neurite extension: an example of designer matrices in tissue engineering. *Faseb J* 1999;13(15):2214–24. [PubMed: 10593869]
12. Patist CM, Mulder MB, Gautier SE, Maquet V, Jerome R, Oudega M. Freeze-dried poly(D,L-lactic acid) macroporous guidance scaffolds impregnated with brain-derived neurotrophic factor in the transected adult rat thoracic spinal cord. *Biomaterials* 2004;25(9):1569–82. [PubMed: 14697859]
13. Iwaya K, Mizoi K, Tessler A, Itoh Y. Neurotrophic agents in fibrin glue mediate adult dorsal root regeneration into spinal cord. *Neurosurgery* 1999;44(3):589–95. [PubMed: 10069596]discussion 95–6
14. Taylor SJ, Rosenzweig ES, McDonald JW 3rd, Sakiyama-Elbert SE. Delivery of neurotrophin-3 from fibrin enhances neuronal fiber sprouting after spinal cord injury. *J Control Release* 2006;113(3):226–35. [PubMed: 16797770]
15. Tsai EC, Dalton PD, Shoichet MS, Tator CH. Matrix inclusion within synthetic hydrogel guidance channels improves specific supraspinal and local axonal regeneration after complete spinal cord transection. *Biomaterials* 2006;27(3):519–33. [PubMed: 16099035]
16. Stokols S, Sakamoto J, Breckon C, Holt T, Weiss J, Tuszynski MH. Templated agarose scaffolds support linear axonal regeneration. *Tissue Eng.* 2006
17. Williams LR. Exogenous fibrin matrix precursors stimulate the temporal progress of nerve regeneration within a silicone chamber. *Neurochem Res* 1987;12(10):851–60. [PubMed: 3683735]
18. Bensaid W, Triffitt JT, Blanchat C, Oudina K, Sedel L, Petite H. A biodegradable fibrin scaffold for mesenchymal stem cell transplantation. *Biomaterials* 2003;24(14):2497–502. [PubMed: 12695076]
19. Sieminski AL, Gooch KJ. Salmon fibrin supports an increased number of sprouts and decreased degradation while maintaining sprout length relative to human fibrin in an in vitro angiogenesis model. *J Biomater Sci Polym Ed* 2004;15(2):237–42. [PubMed: 15109101]
20. Wang LZ, Gorlin J, Michaud SE, Janmey PA, Goddeau RP, Kuuse R, Uibo R, Adams D, Sawyer ES. Purification of salmon clotting factors and their use as tissue sealants. *Thromb Res* 2000;100(6):537–48. [PubMed: 11152934]
21. Becker T, Wullimann MF, Becker CG, Bernhardt RR, Schachner M. Axonal regrowth after spinal cord transection in adult zebrafish. *J Comp Neurol* 1997;377(4):577–95. [PubMed: 9007194]
22. Eitan S, Solomon A, Lavie V, Yoles E, Hirschberg DL, Belkin M, Schwartz M. Recovery of visual response of injured adult rat optic nerves treated with transglutaminase. *Science* 1994;264(5166):1764–8. [PubMed: 7911602]
23. Monsonigo A, Mizrahi T, Eitan S, Moalem G, Bardos H, Adany R, Schwartz M. Factor XIIIa as a nerve-associated transglutaminase. *Faseb J* 1998;12(12):1163–71. [PubMed: 9737719]
24. Wolf, K. Fish viruses and fish viral diseases. Ithaca, NY: Cornell University Press; 1988.
25. Michaud SE, Wang LZ, Korde N, Bucki R, Randhawa PK, Pastore JJ, Falet H, Hoffmeister K, Kuuse R, Uibo R, Herod J, Sawyer E, Janmey PA. Purification of salmon thrombin and its potential as an alternative to mammalian thrombins in fibrin sealants. *Thromb Res* 2002;107(5):245–54. [PubMed: 12479886]
26. Traas DW, Hoegee-de Nobel B, Nieuwenhuizen W. Factors influencing the separation of plasminogen affinity forms I and II by affinity chromatography. *Thromb Haemost* 1984;52(3):347–9. [PubMed: 6531758]
27. Vuento M, Vaheri A. Purification of fibronectin from human plasma by affinity chromatography under non-denaturing conditions. *Biochem J* 1979;183(2):331–7. [PubMed: 534500]

28. Brewer GJ, Torricelli JR, Evege EK, Price PJ. Optimized survival of hippocampal neurons in B27-supplemented Neurobasal, a new serum-free medium combination. *J Neurosci Res* 1993;35(5):567–76. [PubMed: 8377226]
29. Flanagan LA, Chou J, Falet H, Neujahr R, Hartwig JH, Stossel TP. Filamin A, the Arp2/3 complex, and the morphology and function of cortical actin filaments in human melanoma cells. *J Cell Biol* 2001;155(4):511–7. [PubMed: 11706047]
30. Flanagan LA, Rebaza LM, Derzic S, Schwartz PH, Monuki ES. Regulation of human neural precursor cells by laminin and integrins. *J Neurosci Res* 2006;83(5):845–56. [PubMed: 16477652]
31. Mosher DF, Blout ER. Heterogeneity of bovine fibrinogen and fibrin. *J Biol Chem* 1973;248(19):6896–903. [PubMed: 4745449]
32. Georges PC, McCormick M, Flanagan LA, Ju YE, Sawyer E, Janmey P. Tuning the elasticity of biopolymer gels for optimal wound healing. *Mat Res Soc Proc* 2006:897E.
33. Pittier R, Sauthier F, Hubbell JA, Hall H. Neurite extension and in vitro myelination within three-dimensional modified fibrin matrices. *J Neurobiol* 2005;63(1):1–14. [PubMed: 15616962]
34. Pittman RN, Buettner HM. Degradation of extracellular matrix by neuronal proteases. *Dev Neurosci* 1989;11(45):361–75. [PubMed: 2676459]
35. Laidmae I, McCormick ME, Herod JL, Pastore JJ, Salum T, Sawyer ES, Janmey PA, Uibo R. Stability, sterility, coagulation, and immunologic studies of salmon coagulation proteins with potential use for mammalian wound healing and cell engineering. *Biomaterials* 2006;27(34):5771–9. [PubMed: 16919721]
36. Nagata K, Nakajima K, Takemoto N, Saito H, Kohsaka S. Microglia-derived plasminogen enhances neurite outgrowth from explant cultures of rat brain. *Int J Dev Neurosci* 1993;11(2):227–37. [PubMed: 8328303]
37. Tom VJ, Doller CM, Malouf AT, Silver J. Astrocyte-associated fibronectin is critical for axonal regeneration in adult white matter. *J Neurosci* 2004;24(42):9282–90. [PubMed: 15496664]
38. Manseth E, Skjervold PO, Fjaera SO, Brosstad FR, Bjornson S, Flengsrud R. Purification and characterization of Atlantic salmon (*Salmo salar*) fibrinogen. *Comp Biochem Physiol B Biochem Mol Biol* 2004;138(2):169–74. [PubMed: 15193272]
39. Milner R, Campbell IL. The integrin family of cell adhesion molecules has multiple functions within the CNS. *J Neurosci Res* 2002;69(3):286–91. [PubMed: 12125070]
40. Wierzbicka-Patynowski I, Niewiarowski S, Marcinkiewicz C, Calvete JJ, Marcinkiewicz MM, McLane MA. Structural requirements of echistatin for the recognition of alpha(v)beta(3) and alpha(5)beta(1) integrins. *J Biol Chem* 1999;274(53):37809–14. [PubMed: 10608843]
41. Sun L, Zou Z, Collodi P, Xu F, Xu X, Zhao Q. Identification and characterization of a second fibronectin gene in zebrafish. *Matrix Biol* 2005;24(1):69–77. [PubMed: 15749003]
42. Andersen O, Flengsrud R, Norberg K, Salte R. Salmon antithrombin has only three carbohydrate side chains, and shows functional similarities to human beta-antithrombin. *Eur J Biochem* 2000;267(6):1651–7. [PubMed: 10712595]
43. Weisel JW. Fibrinogen and fibrin. *Adv Protein Chem* 2005;70:247–99. [PubMed: 15837518]

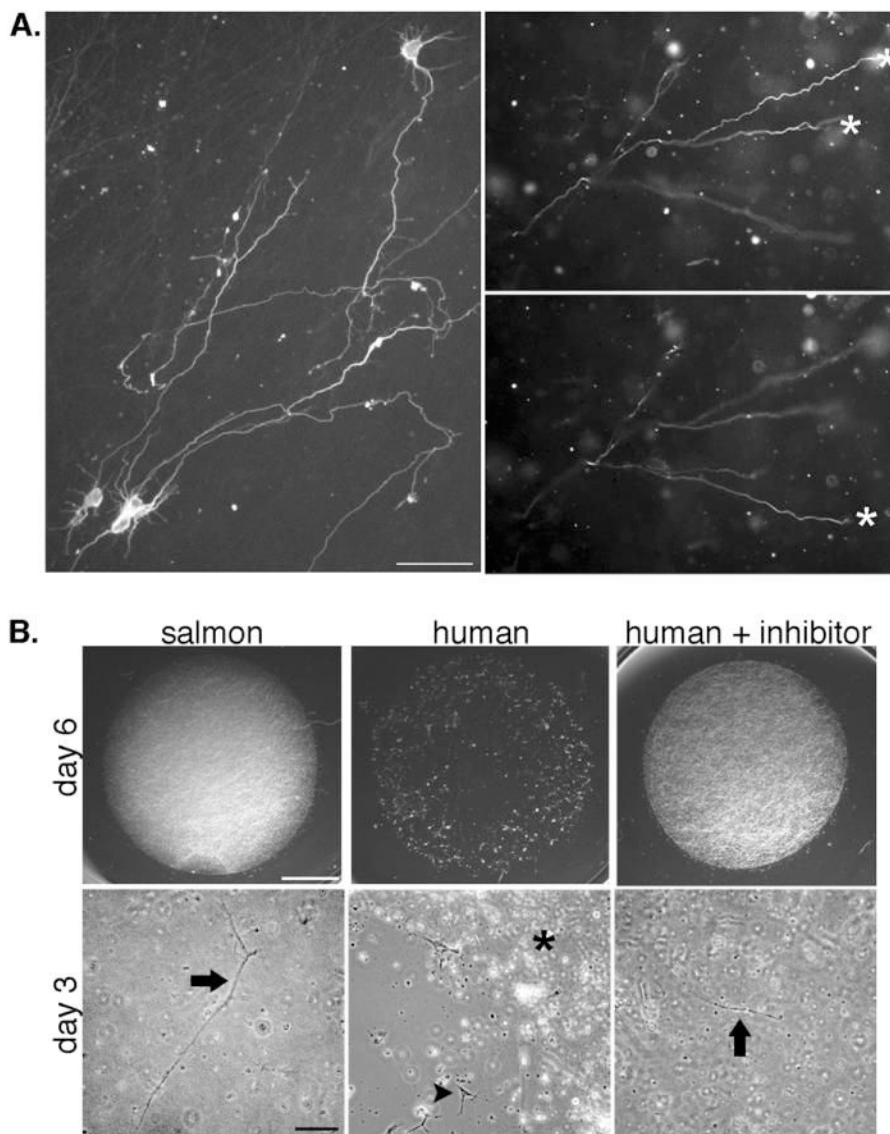


Fig 1. Neurons embedded in fibrin extend neurites in three dimensions and rapidly degrade mammalian fibrin. *A*, Neurons were fixed and immunostained with the neurite marker TuJ1 (which labels both axons and dendrites in embryonic neurons) after growth in gels for 6 days (left panel) or 2 days (right panels). Images of neurites at multiple focal planes were combined in a montage to show the extent of neurite growth (left panel). Right panels show a region of a fibrin gel imaged at two focal planes to demonstrate that neurites have extended in the z-plane. Asterisks mark neurites that are in focus in each plane. Scale bar is 50 μm . *B*, Imaging of the entire gel shows that human gels without plasmin inhibitor are entirely degraded by 6 days (upper panels, scale bar is 200 μm). Higher magnification images of gels at an earlier time point (3 days, lower panels, scale bar is 100 μm) show areas of degradation of the human gels that have left the cells on the coverslip surface (arrowhead, middle panel) next to the residual gel (asterisk). Neurons remain embedded in the salmon fibrin and human fibrin with plasmin inhibitor (arrows).

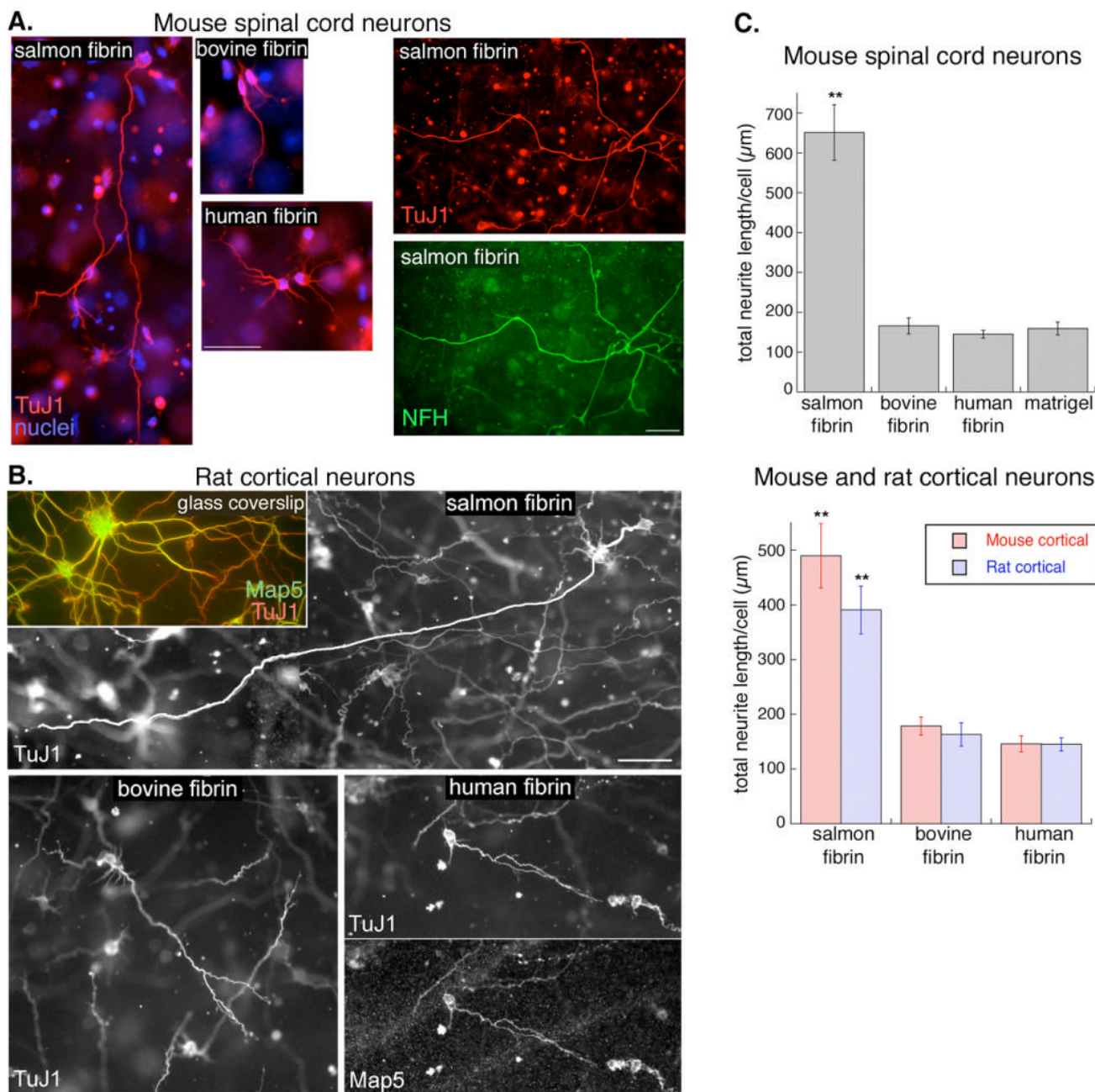


Fig 2. Neurite growth is greater in salmon fibrin than in mammalian fibrin or Matrigel. *A*, Mouse spinal cord neurons embedded in fibrin for 2 days (left 3 panels) or 3 days (right two panels) were immunostained with markers of neurites (TuJ1) or axons (NFH, phosphorylated neurofilament H). Scale bar is 50 μ m. *B*, Rat cortical neurons on laminin-coated glass coverslips or embedded in fibrin for 3 days were immunostained with TuJ1 or Map5/Map1b to visualize neurites. The long neurite in the salmon fibrin has been highlighted to distinguish it from the other neurites in the field (see Supplemental data for the non-highlighted image). Scale bar is 50 μ m. *C*, The effect of the different matrices on neurite growth was quantified by measuring

the total neurite length per cell (** $p < 0.001$ salmon fibrin vs. bovine fibrin, human fibrin, or Matrigel, error bars represent s.e.m.).

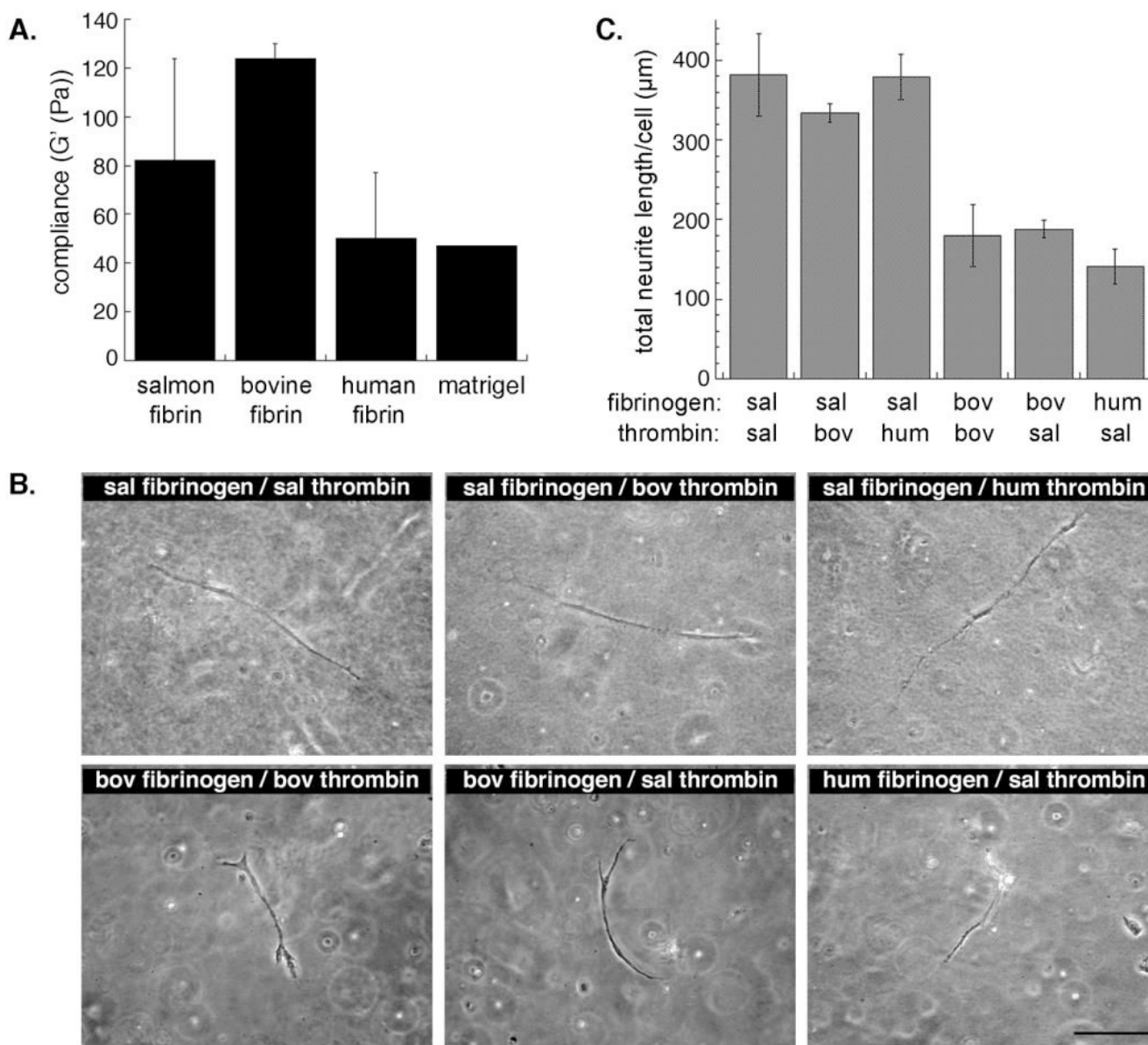


Fig 3. Increased neurite growth in salmon fibrin is not due to differences in matrix compliance or to the species of thrombin. *A*, Shear storage moduli (G') of the fibrin gels and Matrigel are similar and all range from 45-125 Pascals (Pa)(error bars represent s.e.m.). *B*, Fibrin gels were prepared with FBG and thrombin from the same species (controls) or mixed species. Embedded mouse spinal cord neurons were visualized as live cells by phase contrast microscopy after 2 days in the gels (salmon (sal), bovine (bov), human (hum)). Scale bar is 100 μ m. *C*, Total neurite length per cell (mouse spinal cord neurons) was quantified at an early time point (2 days, error bars represent s.e.m.). No significant difference was found among gels prepared with salmon FBG regardless of the species of thrombin and there was no difference among gels containing mammalian FBG polymerized with different thrombins. However, there was a significant difference ($p < 0.01$) between gels containing salmon FBG and those with mammalian FBG.

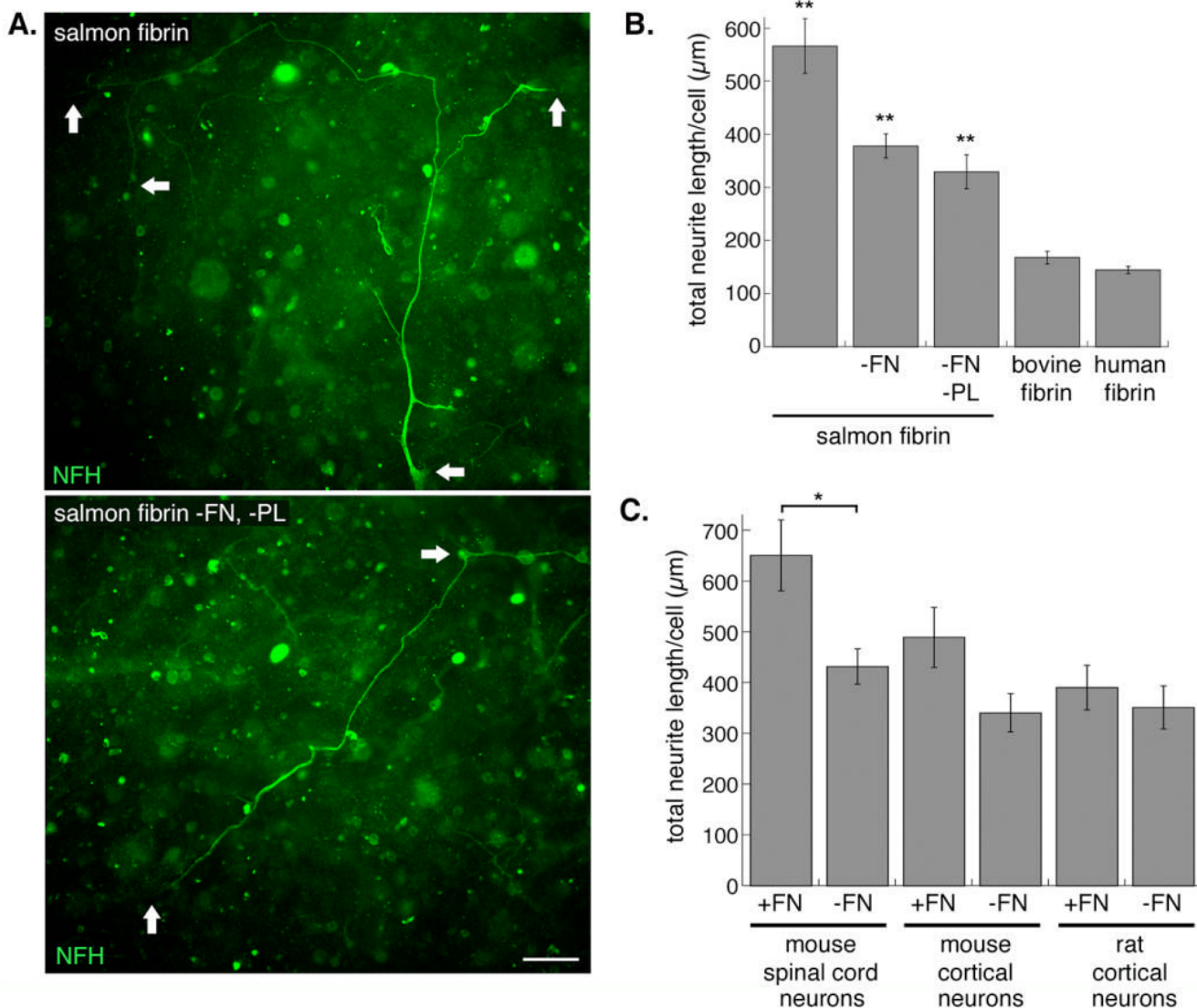


Fig 4. Removal of FN from the salmon FBG component decreases, but does not abolish, the neurite promoting activity. **A**, Mouse spinal cord neurons were embedded in salmon fibrin with (top panel) or without (bottom panel) FN and plasminogen (PL) for 3 days and axons immunostained with anti-NFH (arrows denote neuronal cell bodies and ends of neurites). Scale bar is 50 μm . **B**, The total neurite length per cell was quantified for neurons (combined data from mouse spinal cord and mouse and rat cortical neurons) embedded in control or depleted fibrin gels. Significance levels are as follows: control salmon fibrin vs. salmon fibrin without FN or without FN and PL (** $p < 0.001$); FN-free (or FN- and PL-free) salmon fibrin vs. bovine or human fibrin (** $p < 0.001$) (error bars represent s.e.m.). **C**, Quantification of neurite length for the different types of neurons was separated to show the variation in their responses to FN in the salmon gels (* $p < 0.01$ salmon fibrin with vs. without FN for mouse spinal cord neurons, error bars represent s.e.m.).

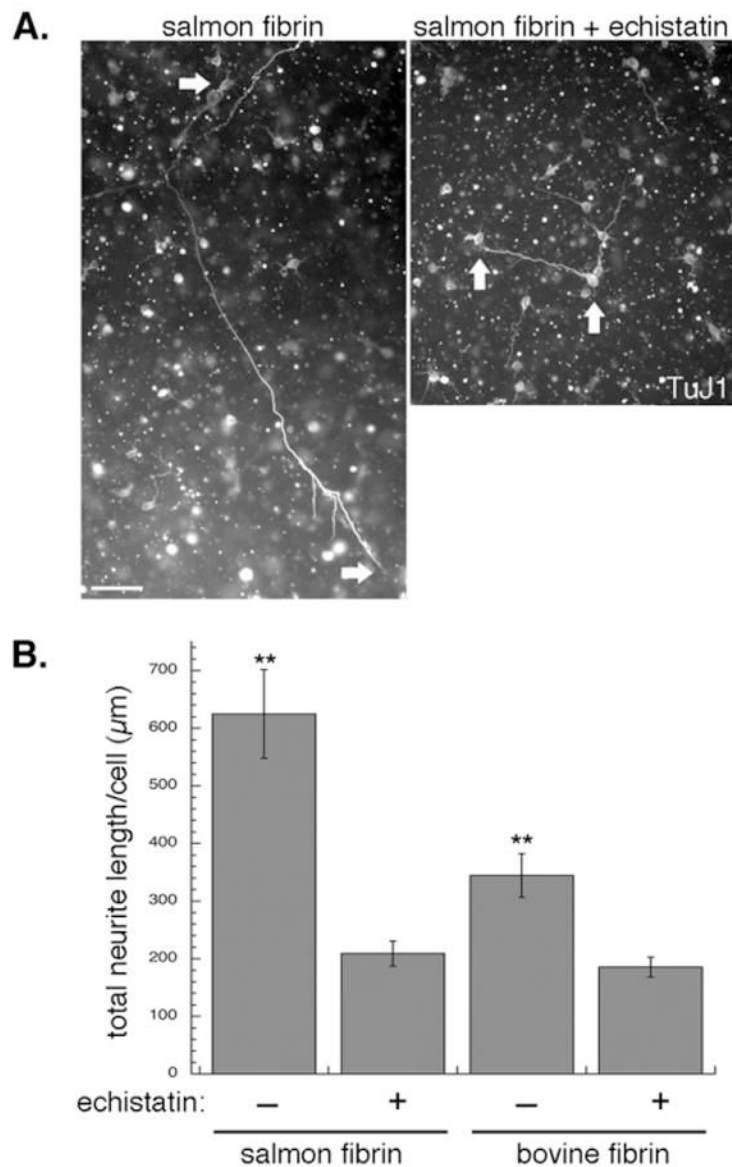


Fig 5. Disruption of FBG/fibrin-integrin binding decreases neurite growth in fibrin. *A*, Mouse spinal cord neurons were embedded in salmon fibrin with and without an integrin inhibitor, echistatin, for 3 days (arrows denote neuronal cell bodies and ends of neurites). Scale bar is 50 μm. *B*, Quantification of neurite growth of mouse spinal cord neurons after 2 days in FN-free salmon fibrin or bovine fibrin with and without echistatin (** $p < 0.001$ echistatin-treated vs. non-treated controls, error bars represent s.e.m.).

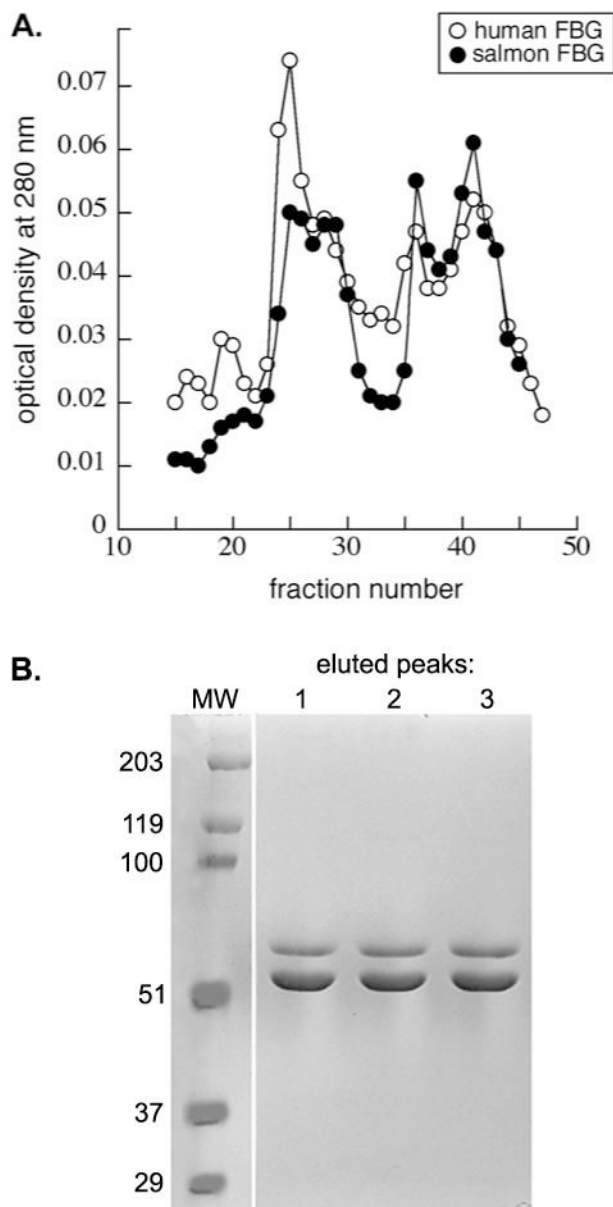


Fig 6. Human and salmon FBG exhibit slightly different anion exchange chromatography profiles. *A*, Elution profiles of human (open circles) and salmon (closed circles) FBG from a DEAE column eluted with a 0-1 M NaCl gradient showed differences in the magnitude of the peaks eluted at low ionic strength. *B*, Peak fractions of the eluted salmon FBG were separated by SDS-PAGE and visualized by coomassie staining.